Fabrication and evaluation of thin layer PVDF composites using MWCNT reinforcement: Mechanical, electrical and enhanced electromagnetic interference shielding properties

B. V. Bhaskara Rao, Nikita Kale, B. S. Kothavale, and S. N. Kale

Citation: AIP Advances **6**, 065107 (2016); doi: 10.1063/1.4953810
View online: http://dx.doi.org/10.1063/1.4953810
View Table of Contents: http://aip.scitation.org/toc/adv/6/6
Published by the American Institute of Physics

Fabrication and evaluation of thin layer PVDF composites using MWCNT reinforcement: Mechanical, electrical and enhanced electromagnetic interference shielding properties

B. V. Bhaskara Rao,[1] Nikita Kale,[2] B. S. Kothavale,[2] and S. N. Kale[1]
[1]*Department of Applied Physics, Defence Institute of Advanced Technology, Pune 411025, India*
[2]*Department of Mechanical Engineering, MAEER's MIT College of Engineering, Pune 411038, India*

(Received 2 May 2016; accepted 30 May 2016; published online 14 June 2016)

Radar X-band electromagnetic interference shielding (EMS) is one of the prime requirements for any air vehicle coating; with limitations on the balance between strength and thickness of the EMS material. Nanocomposite of multiwalled-carbon-nanotubes (MWCNT) has been homogeneously integrated (0 – 9 wt%) with polymer, poly (vinylidene fluoride, PVDF) to yield 300 micron film. The PVDF + 9 wt% MWCNT sample of density 1.41 g/cm^3 show specific shielding effectiveness (SSE) of 17.7 dB/(g/cm^3) (99.6% EMS), with maintained hardness and improved conductivity. With multilayer stacking (900 microns) of these films of density 1.37 g/cm^3, the sample showed increase in SSE to 23.3 dB/(g/cm^3) (99.93% EMS). Uniform dispersion of MWCNTs in the PVDF matrix gives rise to increased conductivity in the sample beyond 5 wt% MWCNT reinforcement. The results are correlated to the hardness, reflection loss, absorption loss, percolation threshold, permittivity and the conductivity data. An extremely thin film with maximum EMS property is hence proposed. © *2016 Author(s). All article content, except where otherwise noted, is licensed under a Creative Commons Attribution (CC BY) license (http://creativecommons.org/licenses/by/4.0/).* [http://dx.doi.org/10.1063/1.4953810]

INTRODUCTION

Carbon-based materials are most intriguing materials for researchers in recent times. Their various forms and types have caught attention due to their exotic properties which find applications in various domains right from sensors to textiles, pharmaceuticals, intelligent coatings and biomedical applications. When such materials are incorporated in polymer matrices to form either composites or doped-polymers or simply carbon-reinforced-polymers, their applications increase multifold, including aerospace structures, sports equipments, automobile spares, organic solar panels, supercapacitors, smart sensors, intelligent painting, electromagnetic interference shielding (EMS) shielding and so on. Amongst these, electromagnetic interference shielding is a well-known issue in scientific electrical/electronic instrumentation, antenna systems and military electronic devices, since the radiation has to be duly shielded to protect a particular entity. Though there has been immense progress done in this particular domain, the materials developed have also had some limitations, on one side; and the applications have posed newer challenges, on the other. Materials such as graphite, carbon black, carbon fibers, carbon nanofibers, carbon nanotubes have been extensively investigated in this context, for EMS owing to their unique combination of electrical conduction, polymeric flexibility, and light weight.[1–5] Interesting theories have been put forth by the researchers to explain the normal and anomalous behavior of carbon-based materials in the various polymer matrices. Percolation theory, negative dielectric materials, metamaterials, micro-capacitors have become new nomenclatures in the domain of EMS materials.[6–9] Enhanced EMS properties of various polymers with carbon-based material-incorporation have been documented by many. Tantis *et al*. have

 ©Author(s) 2016.

explored the functionalized graphene with PVA to form a composite with enhanced electromagnetic shielding.[10] Pande *et al*. have done similar studies with Carbon nanotubes in PMMA matrix to obtain around 40 dB shielding with a few mm-thick materials.[11] Such and other few studies have been done in recent past. However, the ability of the basic polymer material to maintain its mechanical strength intact, and still achieve atleast 95% EMS with minimal thickness of the coating is indeed the challenge. With increased thickness, necessary mechanical strength and EMS property can be achieved; however, the material becomes practically less important, especially for the air-borne applications and coatings. Furthermore, the EMS property has to come with majority of the component from absorption, and not from reflection. This will ensure the stealth application, which is crucial in Radar band, i.e. X-band (8.2-12.4 GHz). Few reports in recent times have been documented upto 50 dB EMS, however, the majority of the component is due to reflectance or thickness; hence not stealth, but other applications can be envisaged.[12] It is due to this that newer materials and synthesis strategies are always in demand to explore a thin coat material, which will provide absorption-dominated EMS materials with no compromise on the mechanical strength of the coat.

In this context, we have synthesized MWCNT-incorporated PVDF thin films of 300 microns thickness using a solvent casting route. The wt % of MWCNT has been varied from 0 to 9 % in the PVDF polymer. The samples have been characterized using X-ray Diffraction (XRD) studies, Fourier transform infrared spectroscopy (FTIR), 4-probe resistivity measurements and field-emission-scanning electron microscopy (FE-SEM) studies. Though FTIR analysis does not confirm any specific conjugation, the XRD data reveals successful incorporation of the MWCNT in the polymer matrix. The conductivity data reveals that the insulating behavior of PVDF shows systematically improved conductivity with MWCNT incorporation, which reaches a threshold at about 5 wt%, beyond which the films become conducting (for 9 wt % films). The data predicts that the MWCNTs establish a percolation path within the PVDF matrix, thereby inducing conductivity. The mechanical hardness of the films do not show degradation upon this incorporation, in fact, shows a slight increase in its Shore "A" value, indicating that the strength of the films gets better. The electromagnetic shielding studies were done using Vector Network Analyzer (PNA N522A ranging from 10 MHz to 26.5 GHz) supported by 85071E material measurement software, shows concomitant increase in the EMS values (from 0.1 dB to 25 dB), especially via the decrease in the S_{21} parameter, which attributes to the absorption (and very less contribution of S_{11}, which is attributed to reflection). The efficiency as high as 99.65% (25 dB) has been observed with single film, which increased to 99.96% (32 dB) with 3 layers of such films, stacked together. These values are highest as reported up-till now for the films as thin as 300 microns for EMS applications, without compromising the mechanical strength of the materials.

EXPERIMENTAL PROCEDURE

Synthesis of PVDF–MWCNT composite film

MWCNT used in these studies were obtained from Global Nanotech Inc., 97% pure, uniform diameter ~15 nm and length ~10–30 μm. Other chemicals were procured from Sigma Aldrich, and were 99.95% pure. PVDF– composite films were synthesized using the solvent casting method.[11] To prepare a composite, the as-synthesized MWCNT were ultrasonically dispersed in toluene for 2 h to obtain a stable suspension of CNTs in toluene. The suspension was then mixed with a solution of PVDF in Dimethyl sulfoxide (DMSO) to obtain a mixture of PVDF–MWCNT with varying wt. % from 0 to 9. The mixture was again ultrasonicated for 2 h to obtain a uniform dispersion of CNTs in PVDF. Thin polymer films were casted from this solution by pouring the solution into a Teflon spray-coated Petri dish (diameter 400) and allowing the solvent to evaporate over 48 hours, followed by drying in an oven. The resulting films had a thickness of about 300 microns and such films of three layers stacking resulted in 900 microns thick films. We report the data here for 0,1,3,5 and 9 wt % MWCNT in PVDF.

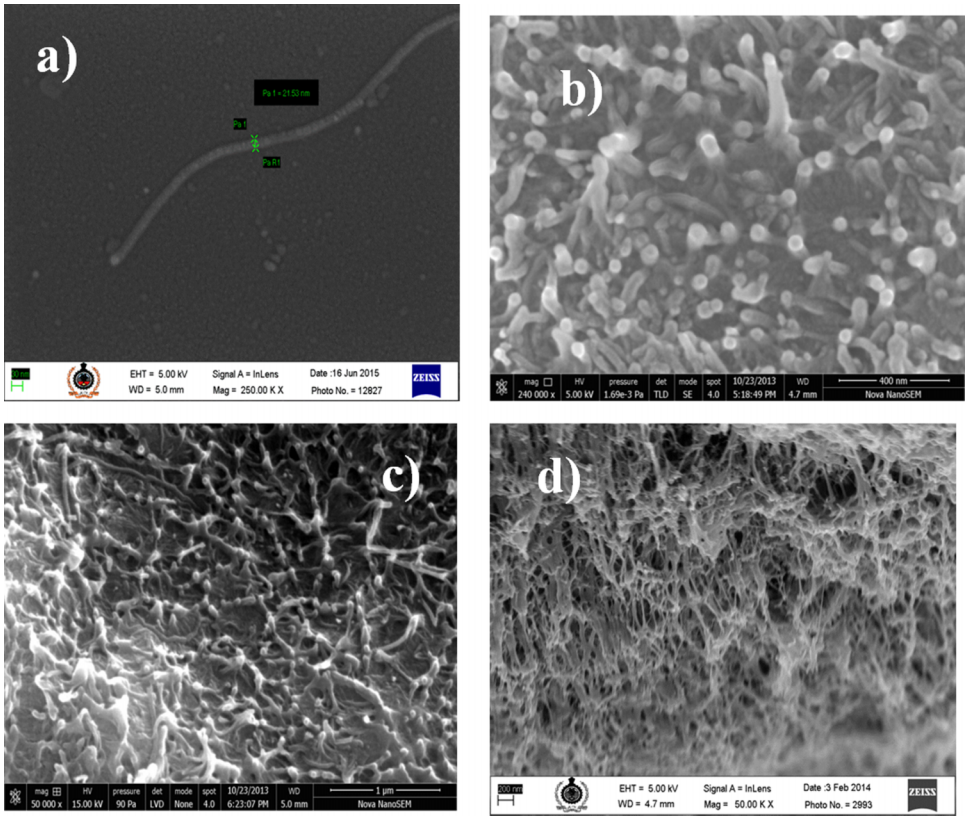

FIG. 1. FE-SEM images of MWCNT in the PVDF matrix. (a) shows a single MWCNT, and images of well dispersed MWCNTs for 3wt%, 5wt% and 9wt% samples in the PVDF matrix are shown in b),c) and d) respectively.

RESULTS AND DISCUSSION

Figure 1 shows the field-emission SEM micrographs of the MWCNTs in PVDF matrix. Figure 1(a) shows a single MWCNT, which has a diameter of around 15 nm. Figures 1(b)-1(d) shows the MWCNTs uniform dispersion and increasing filler concentration in PVDF matrix. Figure 1(d) shows the complex network formation due to high filler concentration.

Figure 2 shows XRD data for PVDF and two specific samples i.e. 3 and 9 wt. % samples in PVDF. The MWCT-incorporated PVDF samples show the signatures of basic polymer. No extra signatures were observed in the MWCNT-incorporated samples. The alpha phases of PVDF films showed four characteristic peaks at the diffraction angles (2θ) of 17.7°, 18.5°, 19.9° and 26.51°, corresponding to (100), (020), (110) and (021) reflections, respectively. The diffraction angle of 20.6° which was assigned to (110) reflection, correspond to the β-phase of crystal, as is also documented earlier.[13,14] Hence the XRD data shows that with MWCNT incorporation there are no visible shifts in the standard PVDF signatures, thereby indicating that the basic structure of polymer is not modified, chemically. Structurally, hence, the system is less strained.

Figure 3 shows the probable conjugational data of the systems. Using the standard data sheets, the characteristic peaks for both phases were identified in both pure as well as MWCNT-incorporated PVDF samples. The α-phase appear at 615 and 760 cm^{-1} (skeletal bending and CF_2 bending), 797 cm^{-1} (CH_2 rocking), and 975 cm^{-1} (CH_2 twisting). On the other hand, the characteristic peaks of the β-crystal phase appear at 840 cm^{-1} (CH_2 rocking) and 1280 cm^{-1} (CF_2 stretching). The peak at 840 cm^{-1}, a characteristic absorption of the β-phase, showed an increase with the amount of MWCNT, while the peaks of α-phase at 615 and 760 cm^{-1} decreased; though not very clearly observed in the FTIR data (Shown in inset of Figure 3). Though it has been mentioned in Refs. 13 and 14, one cannot justify much of conjugation between the PVDF matrix and the MWCNT. However, considering the FE-SEM images and the XRD data, along with

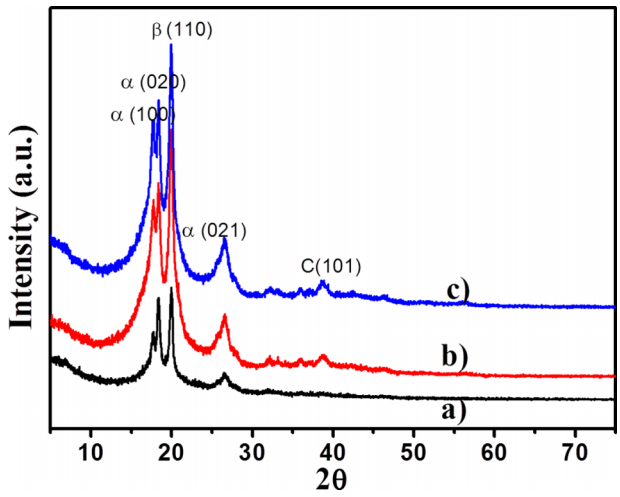

FIG. 2. XRD data of the a)Pure PVDF b) 3 Wt.%+PVDF and c) 9 Wt.%+PVDF.

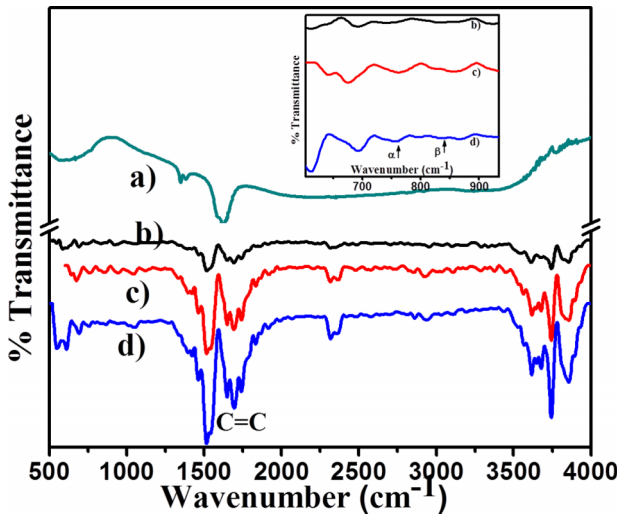

FIG. 3. FTIR data for a) MWCNT b) PVDF c) PVDF with 3wt%MWCNT and d) PVDF with 9wt%MWCNT. The inset shows α and β phases duly elaborated.

this FTIR analysis, it can be concluded that the MWCNTs get incorporated in the PVDF matrix, rather uniformly, without having any chemical conjugation as such. The TGA data confirmed the MWCNT incorporation (by weight) in all the MWCNT-incorporated sample showing that the samples had designated percentage of MWCNT in the PVDF polymer (data not shown). Figure 4 shows the four probe conductivity data which shows encouraging results, from applications point of view. It can be clearly seen that the samples showed high resistivity (open circuit) for the pure PVDF polymer, since it is insulating material. The resistivity falls for 1 wt% MWCNT-incorporated PVDF sample and subsequently for further samples. The sample of 5 wt% MWCNT-incorporated PVDF showed conductivity of 0.023 S/cm, and after that the sample showed further lower values. These values are documented in Table I. The data clearly shows that below 5 wt % incorporation of MWCNT in PVDF, the MWCNTs are not able to connect via a percolation mechanism, thereby offering high resistivity. Beyond 5 wt%, the conductivity does not reduce further and the optimum number of channels available for electrons to flow is established to give good conductivity. This theory of percolation threshold is well documented in the literature, as is also discussed in EMI based materials as well.[11,15–19]

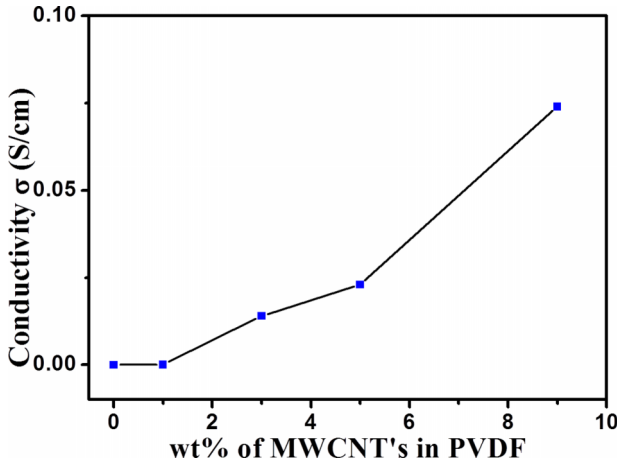

FIG. 4. Conductivity data for all samples which shows a non-linear increase after 5 wt.% MWCNT-PVDF sample.

TABLE I. Summary of all the conductivity, mechanical and electromagnetic shielding data.

S.No	Name of the sample (0.3 mm)	ρ (Ω. cm)	σ (S/cm)	~ε′	~ε″	Tan δ	S.E $_T$ (dB) in X-band for 0.3 mm thick	S.E $_T$ (dB) in X-band for 0.3*3=0.9 mm thick	Shore "A" Hardness
1	PVDF	-	-	1.6	0.04	0.02	0.1	0.1	69.33
2	PVDF+1% MWCNT	19470	0.00005	13	4.5	0.3	2	9	71
3	PVDF+3% MWCNT	69.9	0.014	35	67	1.91	19	23	73
4	PVDF+5% MWCNT	41.7	0.023	27.3	80.8	3	20	28	73
5	PVDF+9% MWCNT	13.5	0.074	-40	93	-2.4	25	32	72.5

Since there was an issue of the hardness compromise with MWCNT incorporation, Shore "A" hardness was measured for all the samples. As has been documented in Table I and Figure 5, pure PVDF showed the value to be 69.33. Upon MWCNT incorporation the value, in fact, improved and reached to 72.5 for the 9 wt % sample, indicating that the sample's mechanical strength did

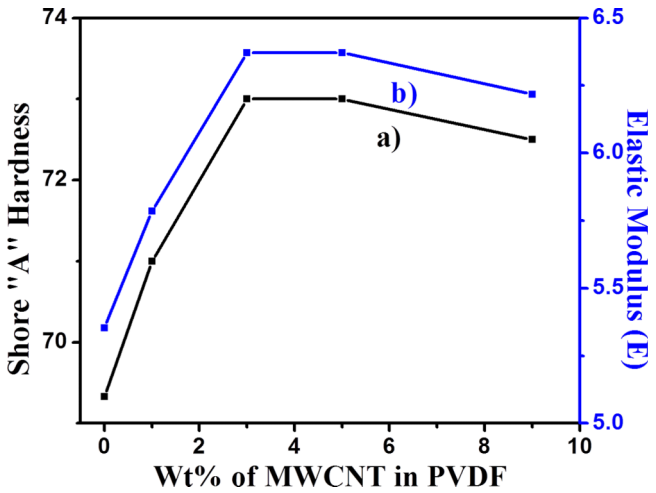

FIG. 5. Hardness data in terms of a) Shore "A" Hardness and b) Elastic modulus (E) values for various MWCNT incorporated PVDF samples.

not suffer with improved conductivity and MWCNT incorporation.[16] The corresponding values of Elastic Modulus (E), given by formula below, show similar trend.

$$E = (0.0981 \times (56 + 7.62336 \times Shore\text{“}A\text{”}))/(0.137505 \times (254 - 2.54 \times Shore\text{“}A\text{”}) \quad (1)$$

The most telling results are shown in Figure 6 and 7. Using VNA setup, various studies were done. First was to evaluate the S_{11} and S_{21} parameters which normally depict the reflection (R) and the absorption (A), respectively, of the radiations in the X-band (8.2-12.4 GHz) by the material.[11,15,17] Using these S_{11} and S_{21} values, the total Shielding effectiveness was calculated using the formula:

$$S.E\,(dB) = -10 * log\,[\frac{P_I}{P_T}] \quad (2)$$

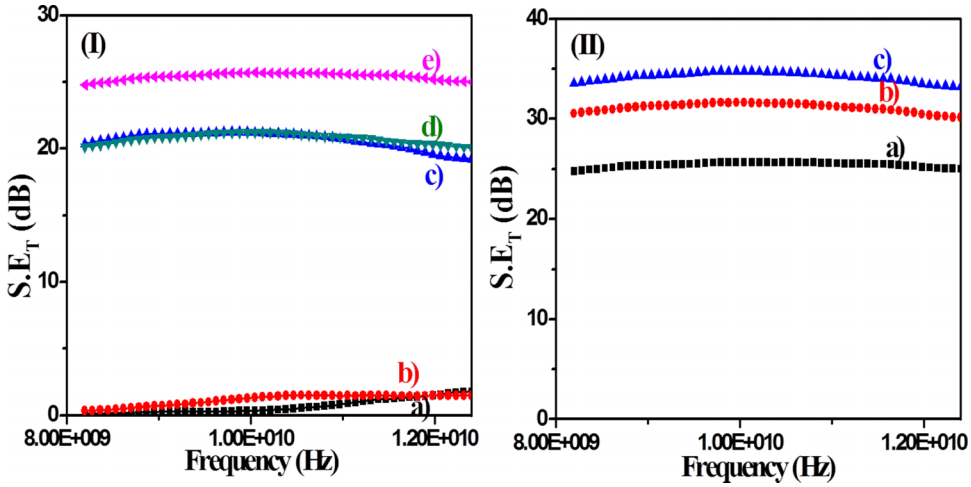

FIG. 6. The Shielding effectiveness data for different samples is shown in Figure 6 (I). (a) PVDF, (b) PVDF+1wt% MWCNT, (c) PVDF+3wt% MWCNT, (d) PVDF+5wt% MWCNT, (e) PVDF+9wt% MWCNT, while Figure 6(II) shows the thickness dependent data for the characteristic 9wt% MWCNT–incorporated PVDF sample of (a) 0.3 mm, (b) 0.6 mm and (c) 0.9 mm.

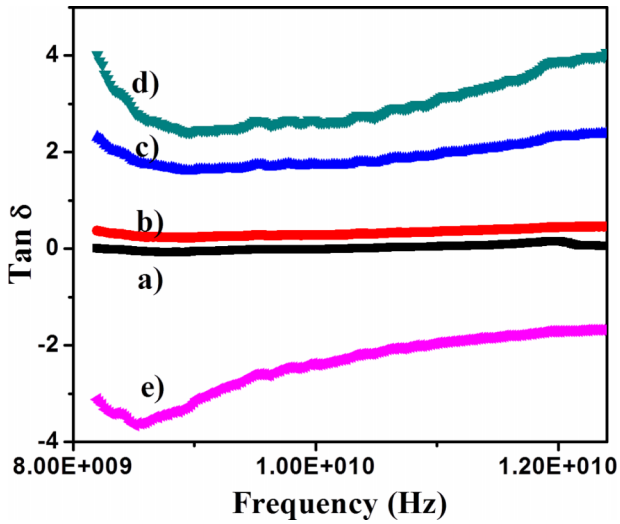

FIG. 7. The Tangent loss (Tan δ) data for (a) PVDF, (b) PVDF+1w% MWCNT, (c) PVDF+3w% MWCNT, (d) PVDF+5w% MWCNT, (e) PVDF+9w% MWCNT of various wt% MWCNT–incorporated PVDF sample.

Where P_I and P_T are Input and Transmit powers respectively.

$$\text{Total shielding effectiveness } S.E\ (dB) = S.E_R + S.E_A + S.E_M \tag{3}$$

Where $R = \mathrm{IS}_{11}\mathrm{I}^2$, $T = \mathrm{IS}_{21}\mathrm{I}^2$, $S.E_R = -10 * log\,(1 - R)$ and $S.E_A = -10 * log\,[\frac{T}{(1-R)}]$

Normally, the loss due to multiple reflections ($S.E_M \sim 0$) is negligible if $\mathrm{S.E}_A$ is >10 dB.

This Shielding effectiveness (SE) in terms of dielectric constant (ε), conductivity (σ′) and permeability (μ′) is given by:

$$S.E_R = -10 * log\,[\frac{\sigma'}{16\omega\mu'\varepsilon_0}] \tag{4}$$

$$S.E_A = -10 * log\,[\frac{\sigma'\omega\mu'}{2}]^{\frac{1}{2}} \text{ where } \sigma' = \varepsilon_o\omega\varepsilon'' \tag{5}$$

$$\text{Tan}\,\delta = \frac{\varepsilon''}{\varepsilon'} \tag{6}$$

Figure 6 (I) shows the SE for all the samples used in these studies. It was clearly observed that the SE values were seen to be extremely low for both pure PVDF and 1wt% MWCNT–incorporated PVDF samples. However for both 3 and 5 wt% MWCNT–incorporated PVDF samples, the SE increased to around 20 dB, and which was seen to increase to the highest value of 25 dB for 9 wt% MWCNT–incorporated PVDF sample. This has been the highest reported values for such samples for mere 300 micron thickness, without compromising the mechanical hardness of the sample. Hence, the samples, especially for the 9 wt% MWCNT–incorporated PVDF were stacked and the layer of 2 and 3 such films was made to obtain a thickness of 600 and 900 microns, respectively. The SE showed further increase to 32 dB with 3 layer stack. These results are shown in Figure 6(b). Though the results for stacking have been shown only for the 9wt% MWCNT–incorporated PVDF sample, all the samples showed similar trend, which is summarized in Table I.

To attribute the results to the explicit role of reflection and / or the absorption modifications in the PVDF base polymer upon MWCNT incorporation, using material measurement software supported by VNA of Transmission/Reflection Line method and the formula shown as (3) and (4) above, the basic parameters of the electromagnetic equation, i.e. ε′ and ε″ were calculated. These are summarized in Table I and Figure 7, which shows the Tan δ parameter shown in equation (5). Dielectric constant (ε′) and corresponding Tan δ values were seen to increase with increasing wt% of MWCNT in PVDF matrix. These values increase up-till 5 wt%, which is the percolation threshold. With higher percentage the value was seen to be negative. Further, for the pure PVDF film, the value of Tanδ was seen to be less than 1, which is also true for 1 wt% doped sample. These films were highly insulating also. Further after 3 wt % the value became ≥1 and later negative at 9 wt%, when the film became highly conducting. The values could be correlated with the conductivity data as well, from Table I.

Looking into various reports[20–28] on materials done earlier, the underneath science was understood. Similar system, such as of PVDF/MWCNT has been studied by G.S. Sudheer *et al.*, which show frequency-dependent results.[28] Gao *et al.*,[22] in their work have done extensive studies on the materials which were made of Fe/Al_2O_3 composites with different Fe volume contents ranging from 10% to 40%. In their studies, they found in the impedance and dielectric properties of these composites, in high frequency range, a distinct dependence on the composition, and the negative permittivity was obtained when Fe content exceeded 20 vol%. They have attributed their results to the negative permittivity from the composites above percolation threshold and the results from Drude model. On similar lines, in our case, PVDF polymer matrix offers an insulator-like dielectric property. As the wt% of MWCNT increases, from 1%, the resistivity is still high, and the material is still insulating. The permittivity and dielectric values are still low. However, at 5wt% loading, the sample approaches the percolation threshold, obtaining optimum conductivity and the loss parameter (obtained from Tan δ) becomes >1. Beyond the threshold, i.e. for 9 wt% sample, the real permittivity switches abruptly. The metal-like negative permittivity behavior is also due to the percolation phenomenon with increasing conducting MWCNT content. Now the conductive component dominates the dielectric properties of the whole MWCNT-incorporated-PVDF matrix. In this case, the dielectric properties of composites transform from insulator-like to metal-like

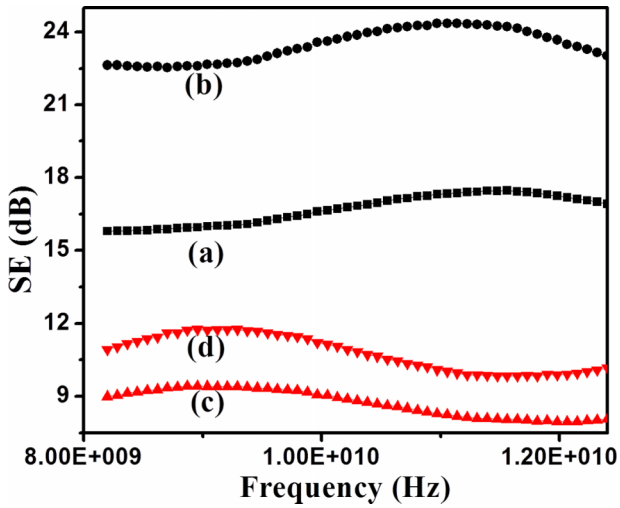

FIG. 8. shows the thickness dependent Shielding Effectiveness by absorption (SE_A) for (a) SE_A of 0.3 mm, (b) SE_A of $0.3\times3=0.9$ mm, and Shielding Effectiveness by reflection (SE_R) for (c) SE_R of 0.3 mm, (d) SE_R of $0.3\times3=0.9$ mm of the PVDF+9wt% MWCNT.

behavior. The real part of complex permittivity undergoes a change not only in magnitude but also in sign. Unlike the insulating PVDF matrix properties, the MWCNTs in the sample tend to connect to each other, and electrons are allowed to make long-range movements.[18–21] Change in ε' (and further Tan δ) from positive to negative after percolation threshold is due to induction polarization.[23–27]

To further evaluate the SE data for all samples and to check whether the high SE is due to reflection and /or absorption, the raw data was again looked into. It was found that, with the incorporation of various wt% of MWCNT in the PVDF, the absorption parameter increased concomitantly in the 5 wt% sample and above, as compared to the reflection contribution. This gave a proof that the material is much lossy, via absorption, basically due to the conducting channels established by MWCNTs in the PVDF matrix. They show this property only after a percolation threshold is achieved, which is at around 5 wt %. The mechanical properties remain intact (even get better), and the samples show excellent EMS properties, via absorption. Figure 8 shows, one such data, as an example, which is for 9 wt% MWCNT–incorporated PVDF sample. The change in the Shielding effectiveness via absorption was seen to be much higher as compared to that Shielding effectiveness via reflection for 1 layer sample of 0.3 mm to 3 layer stack of 0.9 mm thickness. This data indicated that with the reinforcement of MWCNT beyond 5 wt % in the PVDF, the EMS increases to high values, which have the main contribution from the SE_A parameter of the sample, attributed to the radiation absorption. This offers excellent and thin EMS material, which has its mechanical strength intact (and even better).

CONCLUSION

In conclusion, this manuscript demonstrates that in PVDF matrix as MWCNTs concentration increases, SE also increases and for 9 wt% of MWCNTs of 300 microns thick samples, the SE becomes maximum to 25 dB (17.7 dB/(g/cm^3)) which is highest reported; whereas for 3 layers stack it becomes 32 dB (23.3 dB/(g/cm^3)) by improving SE, mainly by absorption. These values are highest as reported up-till now for the films as thin as 300 microns for EMS applications, without compromising the mechanical strength of the materials. The results are attributed the percolation threshold inclusions of MWCNT in PVDF matrix, and further conversion of insulator-to-metallic sample, thereby increasing the loss in the sample due to peculiar permittivity behavior. This loss results in high EMS in the X-band range, which can fetch extremely promising applications in stealth technology.

ACKNOWLEDGEMENT

Authors at DIAT acknowledge funding support of the "DIAT-DRDO Programme on Nanomaterial" and the DIAT-NCL collaboration by ERIPR, DRDO is thankfully acknowledged. All authors also thank Dr. S.B Ogale from IISER-Pune for his guidance to this work.

[1] Z. Spitalsky, D. Tasis, K. Papagelis, and C. Galiotis, Prog. Polym. Sci. **35**, 357 (2010).
[2] D. Cai and M. Song, J. Mater. Chem. **20**, 7906 (2010).
[3] R. Kumar, S. Kumari, and S.R. Dhakate, Appl. Nanosci. **5**, 553 (2014).
[4] M. Chen, L. Zhang, S. Duan, S. Jing, H. Jiang, M. Luo, and C. Li, Nanoscale **6**, 3796 (2014).
[5] H. Kim, A. a. Abdala, and C.W. Macosko, Macromolecules **43**, 6515 (2010).
[6] L.L. Zhang, S. Zhao, X.N. Tian, and X.S. Zhao, Langmuir **26**, 17624 (2010).
[7] B. V. Bhaskara Rao, P. Yadav, R. Aepuru, H.S. Panda, S. Ogale, and S.N. Kale, Phys. Chem. Chem. Phys. **17**, 18353 (2015).
[8] N. Yousefi, X. Sun, X. Lin, X. Shen, J. Jia, B. Zhang, B. Tang, M. Chan, and J.-K. Kim, Adv. Mater. **26**, 5480 (2014).
[9] J. Ling, W. Zhai, W. Feng, B. Shen, J. Zhang, and W. Zheng, ACS Appl.Mater.Interfaces **5**, 2677 (2013).
[10] I. Tantis, Express Polym. Lett. **6**, 283 (2012).
[11] S. Pande, B. Singh, R. Mathur, T. Dhami, P. Saini, and S. Dhawan, Nanoscale Res. Lett. **4**, 327 (2009).
[12] V.K. Singh, A. Shukla, M.K. Patra, L. Saini, R.K. Jani, S.R. Vadera, and N. Kumar, Carbon N. Y. **50**, 2202 (2012).
[13] G.H. Kim, S.M. Hong, and Y. Seo, Phys. Chem. Chem. Phys. **11**, 10506 (2009).
[14] S. Yu, W. Zheng, W. Yu, Y. Zhang, Q. Jiang, and Z. Zhao, Macromolecules **42**, 8870 (2009).
[15] S. Park, P. Theilmann, P. Asbeck, and P.R. Bandaru, IEEE Trans. Nanotechnol. **1** (2009).
[16] S.K. Sharma, R.P. Tandon, and V.K. Sachdev, RSC Adv. **4**, 60733 (2014).
[17] P. Saini, V. Choudhary, B.P. Singh, R.B. Mathur, and S.K. Dhawan, Mater. Chem. Phys. **113**, 919 (2009).
[18] Y. Zhen, J. Arredondo, and G. Zhao, Open J. Org. Polym. Mater. **3**, 99 (2013).
[19] C.A. Martin, J.K.W. Sandler, M.S.P. Shaffer, M.-K. Schwarz, W. Bauhofer, K. Schulte, and A.H. Windle, Compos. Sci. Technol. **64**, 2309 (2004).
[20] R. Aepuru, B.R. B.V., K. SN, and H. Panda, Mater. Chem. Phys. **167**, 61 (2015).
[21] P.-C. Ma, N. a. Siddiqui, G. Marom, and J.-K. Kim, Compos. Part A Appl. Sci. Manuf. **41**, 1345 (2010).
[22] M. Gao, Z. Shi, R. Fan, L. Qian, Z. Zhang, and J. Guo, J. Am. Ceram. Soc. **95**, 67 (2012).
[23] J. Zhu, X. Zhang, N. Haldolaarachchige, Q. Wang, Z. Luo, J. Ryu, D.P. Young, S. Wei, and Z. Guo, J. Mater. Chem. **22**, 4996 (2012).
[24] J. Zhu, S. Wei, L. Zhang, Y. Mao, J. Ryu, P. Mavinakuli, A.B. Karki, D.P. Young, and Z. Guo, J. Phys.Chem. C **114**, 16335 (2010).
[25] X. Zhang, S. Wei, N. Haldolaarachchige, H.A. Colorado, Z. Luo, D.P. Young, and Z. Guo, J. Phys. Chem. C **116**, 15731 (2012).
[26] Y. Tan, H. Luo, H. Zhang, X. Zhou, and S. Peng, AIP ADVANCES **6**, 2158 (2016).
[27] B.P. Singh, V. Choudhary, P. Saini, and R.B. Mathur, AIP ADVANCES **2**, 022151 (2012).
[28] G.S. Kumar, D. Vishnupriya, A. Joshi, S. Datar, and T.U. Patro, Phys. Chem. Chem. Phys. **17**, 20347 (2015).